Eur Radiol (2003) 13:L1–L10
DOI 10.1007/s00330-002-1789-0

Tatsuro Kaminaga
Thoru Takeshita
Izumi Kimura

Role of magnetic resonance imaging for evaluation of tumors in the cardiac region

Received: 4 April 2002
Revised: 17 September 2002
Accepted: 9 December 2002
Published online: 18 January 2003
© Springer-Verlag 2003

T. Kaminaga (✉) · T. Takeshita · I. Kimura
Department of Radiology/Pathology,
Teikyo University Medical School,
2–11–1, Kaga, Itabashi-ku,
1738605 Tokyo, Japan
e-mail: kami@med.teikyo-u.ac.jp
Tel.: +81-3-39644098
Fax: +81-3-53755318

Abstract The aim of this study was to review the role of MRI in the assessment of heart neoplasm, 25 cases with heart neoplasm (10 myxoma, 6 rhabdomyoma, 5 angiosarcoma, 2 mesothelioma, 1 lymphoma, and 1 fibroma) were examined with MRI and echocardiography. Multislice T1- and T2-weighted spin-echo images and static gradient-echo images were taken in appropriate directions with electrocardiogram gating. Gadolinium enhancement was performed in 21 cases. Transthoracic echocardiography was performed in all cases. Except for the 5 patients with rhabdomyoma, the pathological diagnosis was obtained. MRI proved to be useful for tissue characterization of myxoma, angiosarcoma, mesothelioma, and fibroma in cases with tuberous sclerosis. MRI also proved to be useful for detection of the tumor, depiction of contour, relation with other cardiac structures, in cases with myxoma, angiosarcoma, mesothelioma, lymphoma, and fibroma. In the differential diagnosis, MRI provided important information in cases with myxoma, rhabdomyoma, angiosarcoma, and fibroma. In cases with tumors expanding into the mediastinum, such as mesothelioma and fibroma in this report, MRI was useful in determining the location and border. In cases with tumors adjacent to pericardium, MRI was useful in detecting pericardial invasion. Gadolinium enhancement added useful information in cases with myxoma, rhabdomyoma, angiosarcoma, and mesothelioma. The role of MRI with and without Gd enhancement differs somewhat in individual types of heart neoplasm, and adaptation must be considered in each kind of neoplasm. On the other hand, MRI is an essential examination in all cases with a cardiac mass, which has not been diagnosed, since it may provide useful information for the differential diagnosis.

Keywords Heart neoplasm · Magnetic resonance imaging · Gadolinium-DTPA

Introduction

Among the mass lesion originating from cardiac and paracardiac tissue, the most common entity is thrombus, and second is metastasis. Primary heart neoplasm is a rare disease, which is encountered in approximately 0.1% of autopsy cases. Approximately 79–85% of primary heart neoplasms are benign [1, 2, 3, 4, 5]. The most common benign tumor is a myxoma, which is usually attached to the atrial wall. Rhabdomyoma, which always originates from myocardium, and lipoma are secondary common cardiac benign tumors. Among cases with malignant tumor, angiosarcoma, fibrosarcoma, rhabdomyosarcoma, and malignant lymphoma are the most common types. The most common clinical symptoms of patients with heart neoplasm are due to heart failure followed by thromboembolic events, which are characteristically the initial clinical manifestation for myxoma [2].

Improvement in diagnostic technology has increased the number of patients identified with a primary heart neoplasm in its early stage, and has also improved the prognosis. It is established that MRI is a useful method for patients with heart neoplasm. The usefulness of MRI was described regarding the detection of neoplasm [6, 7, 8], depiction of precise neoplasm location, and border and impingement on surrounding structures [6, 7, 8, 9, 10], depiction of neoplasm features that include tissue characterization [6], estimation of the effectiveness of chemotherapy and radiotherapy [10], and differentiation of malignancy from benign tumors [11]. The usefulness of Gd enhancement was also emphasized in this setting [12, 13].

However, the clinical usefulness of MRI is different in each type of heart neoplasm, and adaptation must be discussed in each neoplasm on the basis of clinical experience and reference to the literature. In the present review, 25 patients with myxoma, rhabdomyoma, angiosarcoma, mesothelioma, lymphoma, and fibroma were subjected to MRI examination, and the role of MRI in combination with application of a paramagnetic contrast agent is discussed for each heart neoplasm.

Materials and methods

Twenty-five patients with cardiac tumors (10 myxoma, 6 rhabdomyoma, 5 angiosarcoma, 2 mesothelioma, 1 lymphoma, and 1 fibroma) were examined by MRI and echocardiography. Their age ranged from 2 to 67 years and the male to female ratio was 13 to 12. Except for the 6 patients with rhabdomyoma, surgical/postmortem specimen or autopsy determined the pathological diagnosis. All 6 patients with rhabdomyoma were diagnosed clinically as having tuberous sclerosis.

Electrocardiogram-gated MRI examination was undertaken with 1.5-T super-conducting MRI equipment (Magnetom, Siemens, Erlangen, Germany; Horizon, General Electric Medical Systems, Milwaukee, Wis.). T1- (effective TR/TE: 630±85 ms/22±6 ms) and T2-weighted (effective TR/TE: 1890±295 ms/66±3 ms) spin-echo images (T1 SE, T2 SE) were obtained in all examinations with multislice–multiphase technique. Triggering was performed to every third heart beat on T2 SE. Slice thickness was from 5 to 9 mm and slice gap was 1 mm. Except for 4 patients (1 myxoma, 1 rhabdomyoma, 1 lymphoma, 1 fibroma), Gd enhancement T1-weighted spin-echo imaging was performed with 0.2 ml/kg Magnevist (Japan Shering, Osaka, Japan) intravenous injection. The image interpretation was performed by two trained radiologists individually, and consensus findings were used. The degree of enhancement was classified into high and low grade, when tumors represented superior and equivalent enhancement compared with myocardium. Static gradient-echo (effective TR/TE: 621±62 ms/18±0.2 ms, flip angle 30°) images (GRE) were obtained in 15 patients (10 myxoma and 5 angiosarcoma). The phase image of the GRE sequence was calculated from the same data set in 4 examinations (1 myxoma and 3 angiosarcoma).

Transthoracic echocardiography was performed within 20 days of the MRI examination in all patients. All examinations (MRI and echocardiography) were performed under clinical indications in preparation for surgical operation or to obtain a precise diagnosis.

The interval between surgical operation and MRI examination was 17.4±11.3 days (n=16). All surgical specimens were fixed with formalin and embedded in paraffin for photomicroscopy. Glutaraldehyde-fixed and epon-embedded specimens were prepared for electron microscopy. One trained pathologist decided the diagnosis.

Results

The morphological and MR signal characteristics of each tumor is cumulated in Table 1.

All myxomas were localized in the left atrium and attached to the atrial septum. The MR signal of myxoma was isointense on T1 SE and higher on T2 SE compared with that of normal myocardium and tumors had an irregular contour with heterogeneous signal intensity in-

Table 1 Cumulated morphological and MRI characteristics of each tumor

	Morphology	MR signal intensity			MR signal characteristics		
		T1	T2	Proton	Homogeneous	Enhancement	Special features
Myxoma	Intra-atrial Irregular shaped	Iso	High		No	Weak–strong Irregular	Attachment to atrial septum
Rhabdomyoma	Intra-myocardium Clear contour	Iso	Iso	Mildly high	Yes	Strong Homogeneous	
Angiosarcoma	Intra-arterial Irregular shaped	Iso	High		No	Strong Irregular	"Cauliflower"-appearance Tubular structure with flow void
Mesothelioma	Expansive Intra-pericardial space	Iso	High		T1, yes; T2, no	Strong Irregular	
Lymphoma	Clear contour	Iso	Iso–high		Yes		
Fibroma		Iso	Iso		Yes		

Iso iso signal intensity compared with myocardium; *High* high signal intensity compared with myocardium

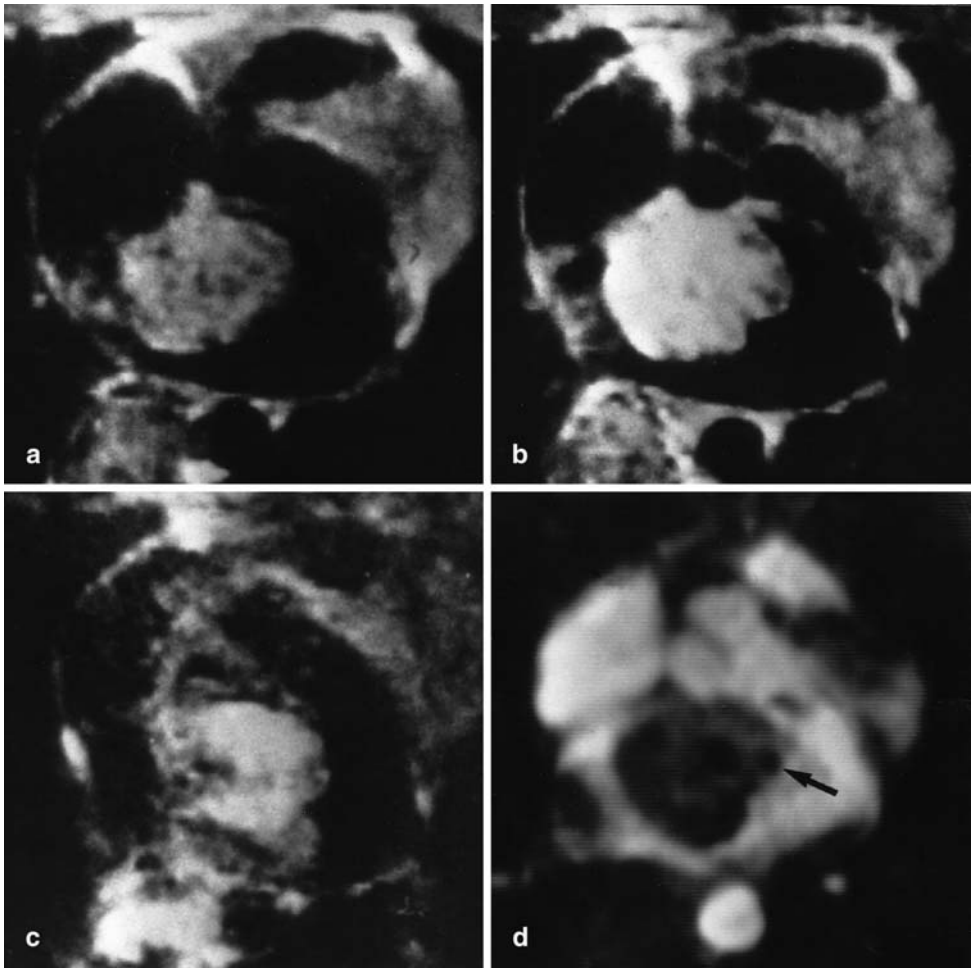

Fig. 1a–d Magnetic resonance imaging of a cardiac myxoma. The signal intensity of the myxoma is isointense on **a** axial T1 spin-echo (SE) with **b** a little heterogeneous enhancement, and hyperintense on **c** axial T2 SE compared with that of normal myocardium. In 2 cases, low signal intensity lesions scattered inside the tumor (*black arrow*) are obvious on **d** axial gradient-echo (GRE) image. The attachment to the atrial wall is well depicted (**a, b, d**)

side on T1 SE, T2 SE, and GRE. All tumors showed heterogeneous enhancement, and three tumors had low, and six tumors had high grade of enhancement.

Echocardiography depicted all of the tumors as heterogeneous echo tumors with attachment to the atrial septum. In 2 cases, low signal intensity lesions were scattered inside the tumor on GRE (Fig. 1). These lesions were echogenic, with corresponding calcifications noted in surgical specimens. The attachment of tumor to atrial wall was well depicted in all cases. The width of the attachment was greater on T1 SE (1.9±1.0 cm) than on GRE (1.7±0.8 cm).

Rhabdomyoma was intramyocardial in 5 cases with prominent extension into the left ventricle in 1 case (Fig. 2). All tumors were homogeneous and isointense on T1 SE and T2 SE compared with normal myocardium. The difference in signal intensity between the tumor and myocardium was emphasized on proton-density-weighted images (Fig. 2). The signal intensity was increased homogeneously with Gd enhancement augmenting signal intensity contrast against normal myocardium in 5 cases (Fig. 2). All tumors were detected with echocardiography. In 1 case, MRI without Gd enhancement could not distinguish the intramyocardial tumor from normal myocardium, whereas echocardiography could detect the tumor in this case. Gadolinium enhancement was not performed in this case because the patient had asthma.

In all 5 patients with angiosarcoma, the signal intensity of the tumors was heterogeneous, and tubular structures with flow-void phenomenon and high-intensity lesions on T1 SE and T2 SE were detected (Fig. 3). On T1 SE, cauliflower appearance [14] was depicted in all cases. The contour was irregular and invasive, and these findings were confirmed by surgical observation. Gadolinium enhancement depicted strong and irregular enhancement. On GRE, low-intensity lesions with strong phase shift were detected (Fig. 3). In surgical specimens, many vascular structures and hemorrhagic lesions were seen inside the tumor. In echocardiography, all tumors were detected as extremely heterogeneous echo masses with irregular contour.

The signal intensity of mesothelioma was homogeneous and similar to that of myocardium on T1 SE, and

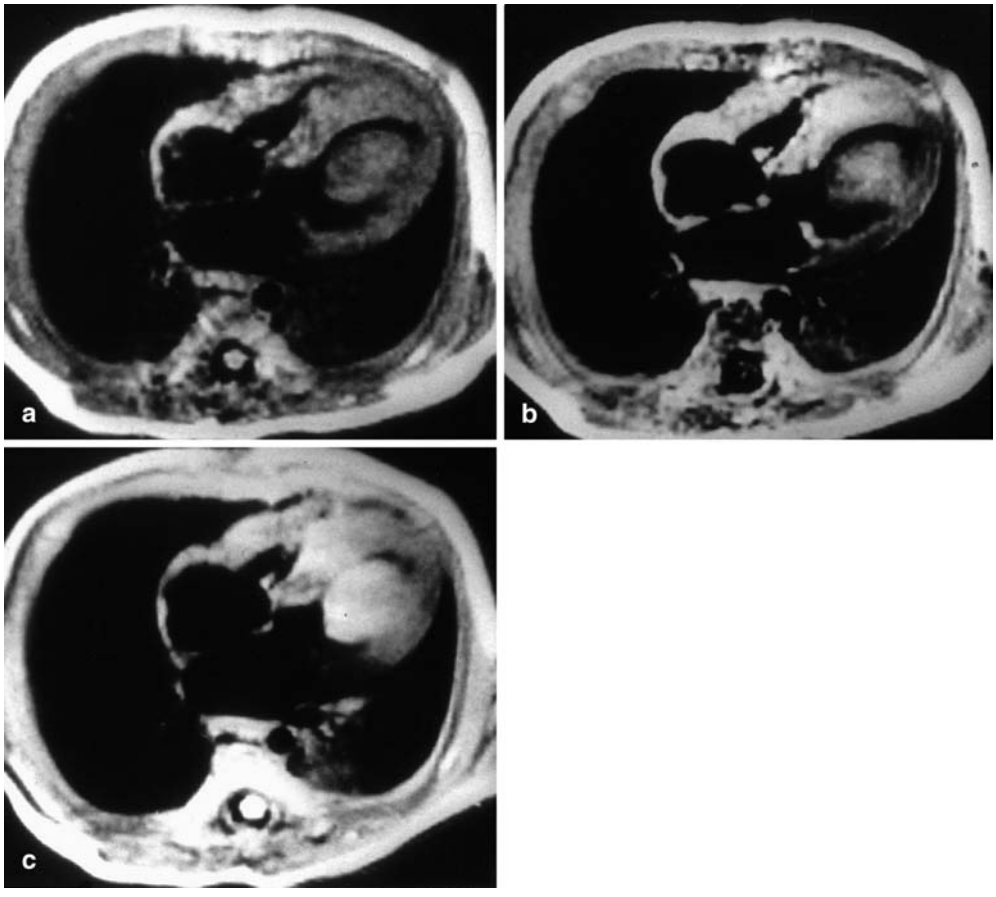

Fig. 2a–c Magnetic resonance imaging of a cardiac rhabdomyoma. The rhabdomyoma is homogeneous and isointense on **a** axial T1 SE. The contrast between the tumor and myocardium is more emphasized on **b** Gd-enhanced image and **c** axial proton-density-weighted image

heterogeneous and higher on T2 SE. This tumor expanded into the pericardial space, and the continuity of the pericardial fat plane surrounding the tumor indicated the non-invasive nature of the tumor to pericardium (Fig. 4). Surgical observation proved the absence of macroscopic invasion to the pericardium, vessels, and cardiac structures. The tumor demonstrated somewhat irregular enhancement with Gd injection, because of the presence of necrotic tissues, proven by examination of the surgical specimen inside the tumor. The border between the tumor and myocardium was initially clarified by Gd enhancement since the tumor was isointense to myocardium on T1 SE (Fig. 4). Echocardiography can detect these tumors as heterogeneous masses; however, it cannot depict whole tumor since a considerable amount of the tumor was in mediastinum. Echocardiography also failed to clarify whether or not the tumor invaded the pericardium.

The pathological diagnosis in this immunocompromised case was non-Hodgkin's lymphoma (diffuse, large B-cell type) based on a post-mortem specimen. No extracardiac lesion was detected. The signal intensity of the lymphoma was the same as other tumors, iso- to slightly hyperintense to myocardium on T1 SE and hyperintense on T2 SE (Fig. 5). The tumor was attached to the wall of the right atrium with prominent extension into the right atrium (Fig. 5). Lobulation was detected on MRI. Thickening of the pericardium was observed indicating tumor involvement of pericardium, but no pericardial effusion was detected. Echocardiography also detected the tumor and the thickening of pericardium in this case.

The signal intensity of fibroma was similar to, and a little higher on, T1- and T2 SE. The tumor was characterized by a relatively low intensity on T2 SE compared with the other cardiac tumors reviewed in this article (Fig. 6). Fibroma also appeared as a homogeneous, well-demarcated tumor on T1 SE and T2 SE. This tumor extended into the pericardial space, and the contour of the tumor was clear. The tumor showed continuity into the anterior myocardium in a limited region, and most parts of the tumor were located in the intrapericardial space (Fig. 6). Echocardiography could not depict the tumor location or its nature precisely in this case, because of limitation of the echo window.

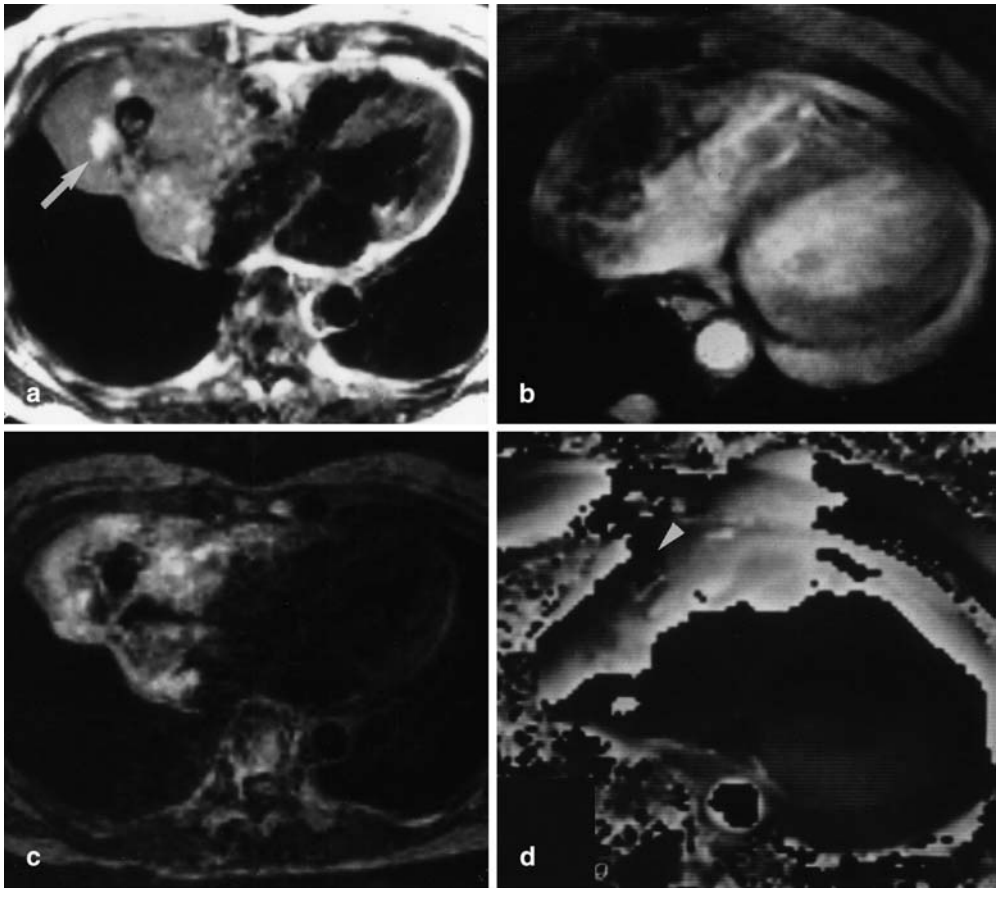

Fig. 3a–d Magnetic resonance imaging of a cardiac angiosarcoma. The signal intensity of this tumor is heterogeneous on **a** axial T1 SE, **b** GRE, and T2 SE with an irregular and invasive contour. Tubular structures with flow-void phenomenon and **c** hyperintense lesions on T1 SE (*arrow*) and T2 SE are detected. On T1 SE, "cauliflower" appearance is depicted in all cases. On GRE, hypointense lesion with strong phase shift (*arrowhead*) on **d** phase image from raw data of image **b** is detected

Discussion

Myxoma

Myxoma usually originates in the left atrium [5, 15, 16, 17, 18, 19] and is attached to the atrial septum. The signal intensity of myxoma is similar to myocardium on T1 SE, and high on T2 SE similar to water, and shows low to high enhancement on Gd-enhanced images as described in a previous report [20]. The signal intensity of myxoma is heterogeneous on T1 SE, T2 SE, and GRE, reflecting the tissue diversity in this tumor [21], such as calcification [22, 23, 24] and hemorrhage. The tumor contour is clearly depicted in all cases; however, on T1 SE and T2 SE, signal arising from slow flow around the tumor precluded distinguishing of the tumor contour. This is the reason why the tumor attachment to the atrial wall was wider on T1 SE than that on GRE (Fig. 1).

The imaging of myxoma is performed mainly by echocardiography, and MRI has a supplemental role [25]. The main role of MRI is tissue characterization [13, 20]. Gadolinium enhancement is not essential for detection of myxoma, since this tumor can easily be depicted on plain T1 and T2 SE, GRE, and especially cine-mode MRI [26].

The differential diagnosis includes thrombus, vegetation, and other tumors. Subacute thrombus has characteristic MR finding [27] and can be differentiated from myxoma. Organized thrombus is more difficult to differentiate, and Gd-enhanced images provide important information [20]. The location within the atrium and existence of a stem are also useful features for the differential diagnosis between thrombus and myxoma. Vegetation can be diagnosed by echocardiography, with some exceptions [28, 29]. Clinical symptoms and/or history are also important for the differential diagnosis.

Rhabdomyoma

In cases with intra-myocardial rhabdomyoma, the contour of the tumor was unclear on T1 and T2 SE without Gd enhancement. Proton-density-weighted images are more useful in distinguishing this tumor from myocardium; however, Gd enhancement is an established method for depiction of the tumor contour. In 1 case, echocardiography proved more sensitive than MRI without Gd en-

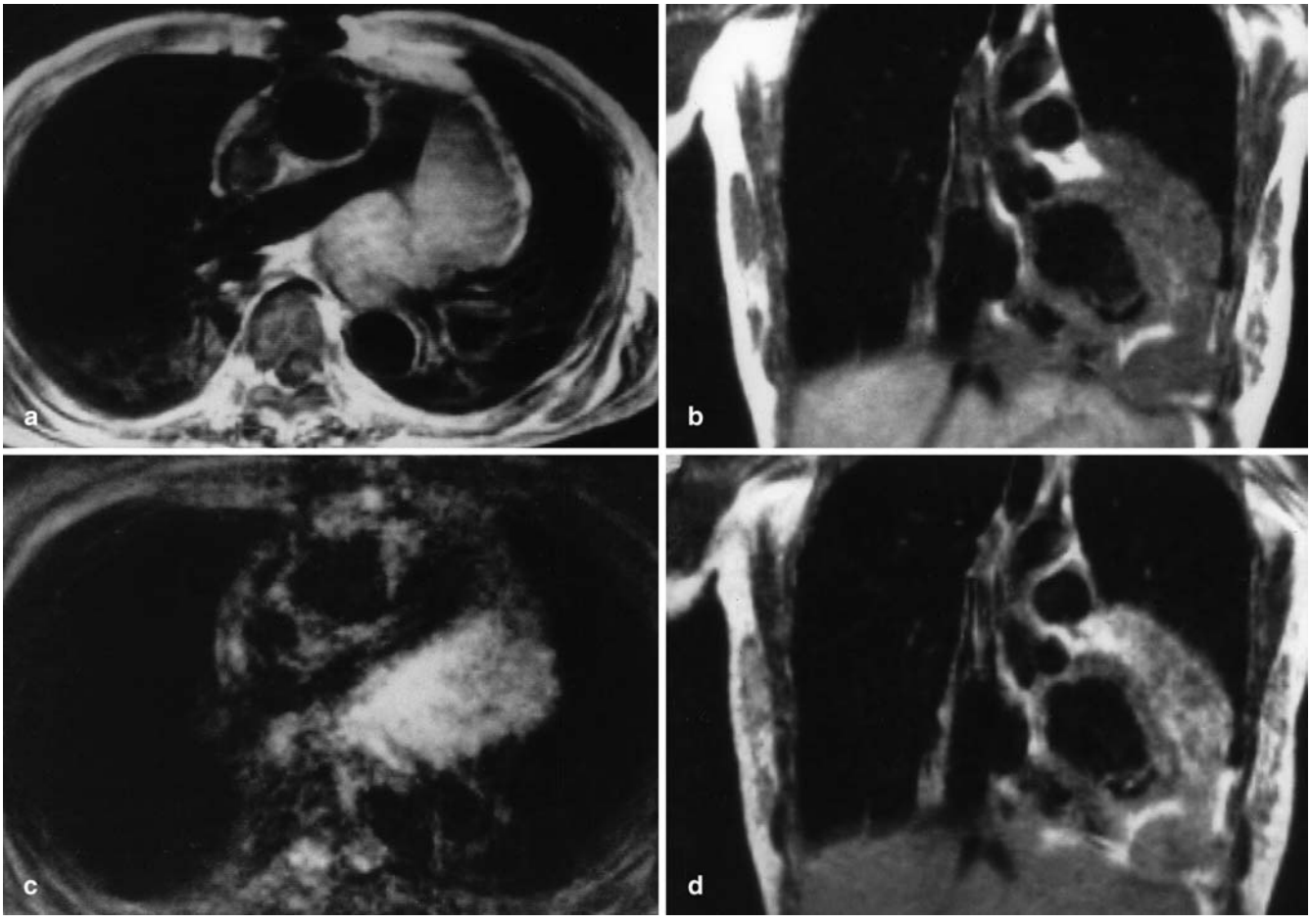

Fig. 4a–d Magnetic resonance imaging of a mesothelioma in cardiac region. The signal intensity of the mesothelioma is homogeneously isointense on **a** axial and **b** coronal T1 SE, and heterogeneously hyperintense on **c** axial T2 SE. This tumor expanded into the pericardial space, and the pericardial fat plane surrounding the tumor was continuous on axial T1 SE. The enhancement was somewhat irregular on **d** coronal Gd-enhanced image. The Gd enhancement was effective in distinguishing the tumor contour from myocardium

hancement for detecting this tumor as was reported by Rienmuller et al. [30]. The echocardiography findings of this tumor are well established and usually no other imaging is needed for the diagnosis [31, 32]; however, Berkenblit et al. reported a case in which MRI was superior to echocardiography in depicting the contour of a rhabdomyoma [33]. Judging from these reports and our own experience, the role of MRI is still limited in the detection of this tumor itself and its border, and is useful when echocardiography fails to depict it.

Among cardiac tumors in cases with tuberous sclerosis, rhabdomyoma is most common, whereas lipoma and fibroma are less frequent [34]. Fibroma has a lower signal intensity on T2 SE compared with that of other tumors. Lipoma shows a characteristic signal intensity from fat tissue [35]. It is possible to distinguish fibroma and lipoma from other tumors according to their characteristic MRI features [36].

Angiosarcoma

Angiosarcoma is the most common primary malignant tumor in the heart. It tends to occur in the right atrium and involve surrounding structures [37]. In our experience, the signal intensity is highly heterogeneous and the same level as normal myocardium on T1 SE and very hyperintense on T2 SE. Tubular structure with flow-void phenomenon represents the vascular structure inside the tumor. The hypointense layer on GRE images with significant phase shift represents susceptibility effect caused by intratumor hemorrhage. These findings were derived from the pathological findings, namely that this tumor has a vascular-rich nature. All these MRI findings were confirmed by pathological examination. Magnetic resonance imaging is superior in depicting the tissue characterization of this tumor. The Gd enhancement depicted strong and irregular enhancement and clearly delineated the tumor margin in our cases. Gadolinum en-

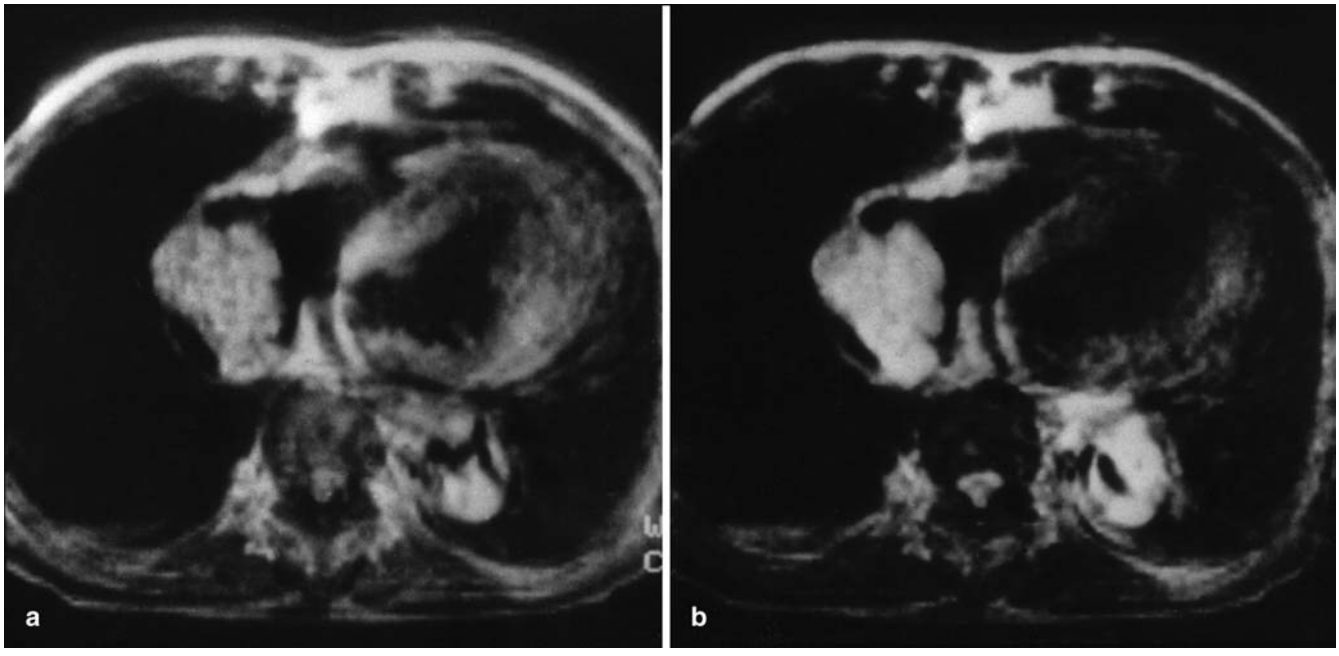

Fig. 5a, b Magnetic resonance imaging of a cardiac lymphoma. The signal intensity of the lymphoma was iso- to slightly hyperintense to myocardium on **a** axial T1 SE and hyperintense on **b** axial T2 SE. Lobulation was detected on MRI. Thickening of the pericardium was observed. No pericardial effusion was detected

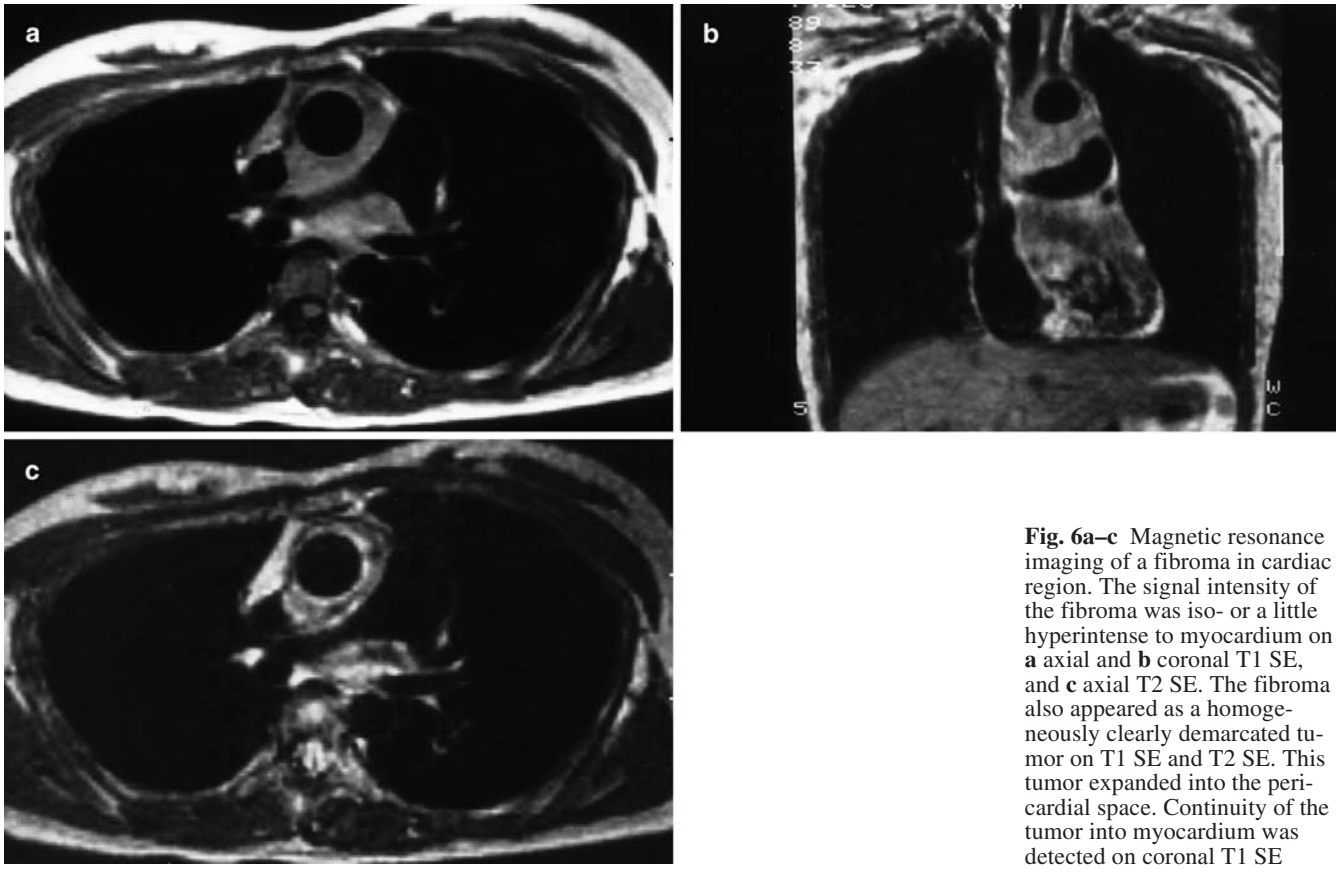

Fig. 6a–c Magnetic resonance imaging of a fibroma in cardiac region. The signal intensity of the fibroma was iso- or a little hyperintense to myocardium on **a** axial and **b** coronal T1 SE, and **c** axial T2 SE. The fibroma also appeared as a homogeneously clearly demarcated tumor on T1 SE and T2 SE. This tumor expanded into the pericardial space. Continuity of the tumor into myocardium was detected on coronal T1 SE

hancement can provide precise information regarding invasion and location of cardiac angiosarcoma. All tumors were also detectable with echocardiography as heterogeneous echo masses with tubular structure in some cases; however, echocardiography is not so suitable for tissue characterization in this tumor compared with MRI.

According to the literature, the MRI features of angiosarcoma include heterogeneous signal intensity originating from intra-tumoral hemorrhage and heterogeneous enhancement [6, 38]. Some unique characteristics on MRI were a cauliflower appearance on T1 SE [14] and a "sun-ray" appearance on enhanced MRI [39]. The differential diagnosis of angiosarcoma is not so difficult recognizing these characteristic features on MRI.

Magnetic resonance imaging is useful for detection, tissue characterization, and localization and diagnosis of this tumor. Echocardiography is also recommendable for detection of the tumor and transesophageal echocardiography facilitates transvenous endomyocardial biopsy of the tumor [40]; however, Inoko et al. [40] and Masauzi et al. [41] have reported cases with angiosarcoma which are detectable with MRI but not with transthoracic echocardiography.

Mesothelioma

According to the literature, mesothelioma from pericardium showed homogeneous isointensity compared with myocardium on T1 SE and greater hyperintensity on T2 SE. The tumor expands into the pericardial space compressing vessels and cardiac structures [8, 42, 43, 44, 45, 46]. These are the characteristic MRI features of this tumor.

The presence of a continuous pericardial fat plane on MRI indicated that there was no macroscopic invasion to the pericardium in our cases, and that was confirmed by surgical findings. On the other hand, invasion to the pericardium is obvious when the hypointense layer of the pericardium is disrupted and/or focal thickening of the pericardium was detected [47, 48]. Magnetic resonance imaging is superior in detecting pericardial invasion of the tumor.

As was reported before [12, 49], Gd enhancement was useful for clarifying the contour between mesothelioma and myocardium in our cases. Gadolinium enhancement is also useful for tissue characterization. Many non-enhanced lesions, which were proved to be necrotic lesions on pathological examination, were detected inside the tumor. Echocardiography failed to detect these necrotic lesions when their diameter was small.

The detection of the tumor was easy by echocardiography; however, it is difficult to depict the whole tumor since the echo window is restricted in the mediastinum, and to determine pericardial invasion, by echocardiography. Computed tomography and/or MRI are essential to determine tumor location and extent in cases with mediastinum tumor. As for tissue characterization, Gd-enhanced MRI is more suitable compared with echocardiography.

Lymphoma

Cardiac lymphoma tends to arise from the right chambers of the heart [50]. In our case, the tumor with lobulation also arose from the right atrium. Magnetic resonance imaging can depict tumor location and morphology precisely. It also depicted the pericardial involvement as thickening of the pericardium, a finding frequently noted in cardiac lymphoma [6]. The differential diagnosis is difficult with MRI alone, since the MR features of this tumor are not specific. It is also difficult with other imaging modalities, and so thoracotomy, or autopsy or cytological examination of pericardial effusion fluid [51], is essential for the diagnosis. Judging from the literature, the major role of MRI for cardiac lymphoma is tumor detection. Ceresoli et al. reported that MRI has a >90% sensitivity for the detection of cardiac lymphoma [50].

Fibroma

Fibroma is the second most common benign cardiac tumor in childhood [52], and its differentiation from rhabdomyoma, which is the most common cardiac benign tumor in childhood, is important. The signal intensity of cardiac fibroma was the same as reported before [52, 53, 54], namely iso- to a little hyperintense compared with myocardium on T1 SE and hypointense on T2 SE. Burke et al. [52] and Araoz et al. [53] also reported the hypointensity of cardiac fibroma on T2 SE. This relative hypointensity reflects the abundant fibrous tissue inside the tumor [55] and is useful for differentiation from rhabdomyoma. Tazelaar et al. [56] and Basso et al. [57] reported that dystrophic calcification is commonly detected in cardiac fibroma. The presence of calcification is another important point in the differentiation from rhabdomyoma [58].

This tumor expanded into the pericardial space with a little attachment to the left ventricular myocardium. Almost all fibromas arise from the left ventricular area [52], and to our knowledge, neither cardiac fibroma arising from pericardial tissue nor ones extending from the myocardium into the pericardial space have been reported. The usefulness of Gd enhancement is not established for cardiac fibroma. In this case, echocardiography was not suitable for tumor observation because of the "narrow" echo window, which is one of major defects of this modality.

In general, MRI is one of the most powerful tools for detection, differential diagnosis, and tissue characteriza-

tion of cardiac tumors. It is essential in cases with an undiagnosed cardiac mass, since it will provide useful information for the differential diagnosis. Echocardiography is commonly used and is suitable as the first imaging modality of cardiac tumors, since it is inexpensive and convenient. Furthermore, it can depict moving pictures and is not affected by paramagnetic metals. The general benefits of MRI over echocardiography are large field of view, multiplanar imaging capabilities, reproducible image quality, no restriction of access due to mediastinal structures, and independence from skill of physicians. The usefulness of cine MRI must be mentioned for providing moving pictures. As reported previously [26, 59], it can depict tumor movement and can increase detectability of tumors. The role of Gd enhancement is summarized as follows: differential diagnosis from organized thrombus in myxoma cases; depiction of the tumor and its contour in rhabdomyoma cases; delineation of the tumor margin in angiosarcoma cases; and clarifying tumor contour against myocardium and tissue characterization in mesothelioma cases.

References

1. Meng Q, Lai H, Lima J, Tong W, Qian Y, Lai S (2002) Echocardiographic and pathologic characteristics of primary cardiac tumors: a study of 149 cases. Int J Cardiol 84:69–75
2. Endo A, Ohtahara A, Kinugawa T, Nawada T, Fujimoto Y, Mashiba H, Shigemasa C (1996) Clinical incidence of primary cardiac tumors. J Cardiol 28:227–234
3. Perchinsky MJ, Lichtenstein SV, Tyers GF (1997) Primary cardiac tumors: 40 years' experience with 71 patients. Cancer 79:1809–1815
4. Grande AM, Ragni T, Vigano M (1993) Primary cardiac tumors. A clinical experience of 12 years. Tex Heart Inst J 20:223–230
5. Molina JE, Edwards JE, Ward HB (1990) Primary cardiac tumors: experience at the University of Minnesota. Thorac Cardiovasc Surg 38 (Suppl) 2:183–191
6. Araoz PA, Eklund HE, Welch TJ, Breen JF (1999) CT and MR imaging of primary cardiac malignancies. Radiographics 19:1421–1434
7. Brown JJ, Barakos JA, Higgins CB (1989) Magnetic resonance imaging of cardiac and paracardiac masses. J Thorac Imaging 4:58–64
8. Hoffmann U, Globits S, Frank H (1998) Cardiac and paracardiac masses. Current opinion on diagnostic evaluation by magnetic resonance imaging. Eur Heart J 19:553–563
9. Amparo EG, Higgins CB, Farmer D, Gamsu G, McNamara M (1984) Gated MRI of cardiac and paracardiac masses: initial experience. AJR 143:1151–1156
10. Schvartzman PR, White RD (2000) Imaging of cardiac and paracardiac masses. J Thorac Imaging. 15:265–273
11. Siripornpitak S, Higgins CB (1997) MRI of primary malignant cardiovascular tumors. J Comput Assist Tomogr 21:462–466
12. Funari M, Fujita N, Peck WW, Higgins CB (1991) Cardiac tumors: assessment with Gd-DTPA enhanced MR imaging. J Comput Assist Tomogr 15:953–958
13. Matsuoka H, Hamada M, Honda T, Kawakami H, Abe M, Shigematsu Y, Sumimoto T, Hiwada K (1996) Morphologic and histologic characterization of cardiac myxomas by magnetic resonance imaging. Angiology 47:693–698
14. Kim EE, Wallace S, Abello R, Coan JD, Ewer MS, Salem PA, Ali MK (1989) Malignant cardiac fibrous histiocytomas and angiosarcomas: MR features. J Comput Assist Tomogr 13:627–632
15. Moosdorf R, Scheld HH, Hehrlein FW (1990) Tumors of the heart. Experiences at the Giessen University Clinic. Thorac Cardiovasc Surg 38 (Suppl 2):208–210
16. Li GY (1990) Incidence and clinical importance of cardiac tumors in China: review of the literature. Thorac Cardiovasc Surg 38 (Suppl 2):205–207
17. Sezai Y (1990) Tumors of the heart. Incidence and clinical importance of cardiac tumors in Japan and operative technique for large left atrial tumors. Thorac Cardiovasc Surg 38 (Suppl 2):201–204
18. Tschirkov A, Michev B, Topalov V, Michailov D, Jurukova Z, Petkov R (1990) Incidences and surgical aspects of cardiac myxomas in Bulgaria. Thorac Cardiovasc Surg 38 (Suppl 2):196–200
19. Blondeau P (1990) Primary cardiac tumors: French studies of 533 cases. Thorac Cardiovasc Surg 38 (Suppl 2):192–195
20. Sommer T, Vahlhaus C, Hofer U, Smekal A von, Wardelmann E, Bierhoff E, Pauleit D, Wilhelm K, Textor J, Schild H (1999) MRI diagnosis of cardiac myxomas: sequence evaluation and differential diagnosis. Rofo Fortschr Geb Rontgenstr Neuen Bildgeb Verfahr 170:156–162
21. Burke AP, Virmani R (1993) Cardiac myxoma. A clinicopathologic study. Am J Clin Pathol 100:671–680
22. Pucillo AL, Schechter AG, Kay RH, Moggio R, Herman MV (1990) Identification of calcified intracardiac lesions using gradient echo MR imaging. J Comput Assist Tomogr 14:743–747
23. de Roos A, Weijers E, van Duinen S, van der Wall EE (1989) Calcified right atrial myxoma demonstrated by magnetic resonance imaging. Chest 95:478–479
24. Masui T, Takahashi M, Miura K, Naito M, Tawarahara K (1995) Cardiac myxoma: identification of intratumoral hemorrhage and calcification on MR images. AJR 164:850–852
25. Reynen K (1995). Cardiac myxomas. N Engl J Med 333:1610–1617
26. Spuentrup E, Kuehl HP, Wall A, Heer C, Buecker A (2001). Visualization of cardiac myxoma mobility with real-time spiral magnetic resonance imaging. Circulation 104:E101–E111
27. Paydarfar D, Krieger D, Dib N, Blair RH, Pastore JO, Stetz JJ Jr, Symes JF (2001) In vivo magnetic resonance imaging and surgical histopathology of intracardiac masses: distinct features of subacute thrombi. Cardiology 95:40–47
28. Siwach SB, Katyal VK, Jagdish (1999) Intracardiac mass lesions: experience of 14 cases. Indian Heart J 51:414–417
29. Child JS, MacAlpin RN, Moyer GH, Shanley JD, Layfield LJ (1979) Coronary ostial embolus and mitral vegetation simulating a left atrial myxoma: a case of probable cryptococcal valvulitis. Clin Cardiol 2:43–48
30. Rienmuller R, Lloret JL, Tiling R, Groh J, Manert W, Muller KD, Seifert K (1989) MR imaging of pediatric cardiac tumors previously diagnosed by echocardiography. J Comput Assist Tomogr 13:621–626

31. Sallee ML, Spector DW, van Heeckeren, Patel CR (1999) Primary pediatric cardiac tumors: a 17 year experience. Cardiol Young 9:155–162
32. Wann LS, Sampson C, Liu Y (1998) Cardiac and paracardiac masses: complementary role of echocardiography and magnetic resonance imaging. Echocardiography 15:139–146
33. Berkenblit R, Spindola-Franco H, Frater RW, Fish BB, Glickstein JS (1997) MRI in the evaluation and management of a newborn infant with cardiac rhabdomyoma. Ann Thorac Surg 63:1475–1477
34. Donegani G (1972) Tuberous sclerosis. Handbook of clinical neurology, vol 14. North Holland Publishers, Amsterdam, pp 340–349
35. Mousseaux E, Idy-Peretti I, Bittoun J, Diebold B, Paulylaubry C, Carpentier A, Gaux JC (1992) MR tissue characterization of a right atrial mass: diagnosis of a lipoma. J Comput Assist Tomogr 16:148–151
36. Matsumura M, Nishioka K, Yamashita K, Yoshibayashi M, Okuno T, Konishi J, Shimizu T, Temma S, Ueda T, Mikawa H (1991) Evaluation of cardiac tumors in tuberous sclerosis by magnetic resonance imaging. Am J Cardiol 68:281–283
37. Janigan DT, Husain A, Robinson NA (1986) Cardiac angiosarcomas. A review and a case report. Cancer 57:852–859
38. Bruna J, Lockwood M (1998) Primary heart angiosarcoma detected by computed tomography and magnetic resonance imaging. Eur Radiol 8:66–68
39. Yahata S, Endo T, Honma H, Ino T, Hayakawa H, Ogawa M, Hayashi H, Kumazaki T (1994) Sunray appearance on enhanced magnetic resonance image of cardiac angiosarcoma with pericardial obliteration. Am Heart J 127:468–471
40. Inoko M, Iga K, Kyo K, Kondo H, Tamura T, Izumi C, Kitagichi S, Hirozane T, Himura Y, Gen H, Konishi T (2001) Primary cardiac angiosarcoma detected by magnetic resonance imaging but not by computed tomography. Intern Med 40:391–395
41. Masauzi N, Ichikawa S, Nishimura F, Yoshino Y, Mihara J, Hayama Y, Shimazaki E, Kawase I, Toyama M, Kokubo T (1992) Primary angiosarcoma of the right atrium detected by magnetic resonance imaging. Intern Med 31:1291–1297
42. Kaminaga T, Yamada N, Imakita S, Takamiya M, Nishimura T (1993) Magnetic resonance imaging of pericardial malignant mesothelioma. Magn Reson Imaging 11:1057–1061
43. Gossinger HD, Siostrzonek P, Zangeneh M, Neuhold A, Herold C, Schmoliner R, Laczkovics A, Tscholakoff D, Mosslacher H (1988) Magnetic resonance imaging findings in a patient with pericardial mesothelioma. Am Heart J 115:1321–1322
44. Vogel HJ, Wondergem JH, Falke TH (1989) Mesothelioma of the pericardium: CT and MR findings. J Comput Assist Tomogr 13:543–546
45. Shimojo M, Tsuda N, Kamihata H, Inada M, Kato T, Sawada S, Tanaka Y (1989) Magnetic resonance imaging for cardiovascular masses. J Cardiology 19:583–592
46. Gossinger HD, Siostrzonek P, Zangeneh M, Neuhold A, Herold C, Schmoliner R, Laczkovics A, Tscholakoff D, Mosslacher H (1988) Magnetic resonance imaging findings in a patient with pericardial mesothelioma. Am Heart J 115:1321–1322
47. White CS (1996) MR evaluation of the pericardium and cardiac malignancies. Magn Reson Imaging Clin N Am 4:237–251
48. Barakos JA, Brown JJ, Higgins CB (1989) MR imaging of secondary cardiac and paracardiac lesions. Am J Roentgenol 153:47–50
49. Niwa K, Tashima K, Terai M, Okajima Y, Nakajima H (1989) Contrast-enhanced magnetic resonance imaging of cardiac tumors in children. Am Heart J 118:424–425
50. Ceresoli GL, Ferreri AJ, Bucci E, Ripa C, Ponzoni M, Villa E (1997) Primary cardiac lymphoma in immunocompetent patients: diagnostic and therapeutic management. Cancer 80:1497–1506
51. Pozniak AL, Thomas RD, Hobbs CB, Lever JV (1986) Primary malignant lymphoma of the heart. Antemortem cytologic diagnosis. Acta Cytol 30:662–664
52. Burke AP, Rosado de Christenson M, Templeton PA, Virmani R (1994) Cardiac fibroma: clinicopathologic correlates and surgical treatment. J Thorac Cardiovasc Surg 108:862–870
53. Araoz PA, Mulvagh SL, Tazelaar HD, Julsrud PR, Breen JF (2000) CT and MR imaging of benign primary cardiac neoplasms with echocardiographic correlation. Radiographics 20:1303–1319
54. Parmley LF, Salley RK, Williams JP, Head GB III (1988) The clinical spectrum of cardiac fibroma with diagnostic and surgical considerations: noninvasive imaging enhances management. Ann Thorac Surg 45:455–465
55. de Montpreville VT, Serraf A, Aznag H, Nashashibi N, Planche C, Dulmet E (2001) Fibroma and inflammatory myofibroblastic tumor of the heart. Ann Diagn Pathol 5:335–342
56. Tazelaar HD, Locke TJ, McGregor CG (1992) Pathology of surgically excised primary cardiac tumors. Mayo Clin Proc 67:957–965
57. Basso C, Valente M, Poletti A, Casarotto D, Thiene G (1997) Surgical pathology of primary cardiac and pericardial tumors. Eur J Cardiothorac Surg 12:730–737
58. Beghetti M, Gow RM, Haney I, Mawson J, Williams WG, Freedom RM (1997) Pediatric primary benign cardiac tumors: a 15-year review. Am Heart J 134:1107–1114
59. Wintersperger BJ, Becker CR, Gulbins H, Knez A, Bruening R, Heuck A, Reiser MF (2000) Tumors of the cardiac valves: imaging findings in magnetic resonance imaging, electron beam computed tomography, and echocardiography. Eur Radiol 10:443–449